Electron-impact ionization excitation of helium in the quasiphoton regime

J. M. Ngoko Djiokap,[1,2] E. Foumouo,[2] M. G. Kwato Njock,[1] X. Urbain,[2] and B. Piraux[2,*]

[1]*Centre for Atomic, Molecular Physics and Quantum Optics, Faculty of Science, University of Douala, Post Office Box 8580, Douala, Cameroon*

[2]*Institute of Condensed Matter and Nanosciences, Université catholique de Louvain, Bâtiment de Hemptinne, 2 chemin du cyclotron, B1348 Louvain-la Neuve, Belgium*

(Received 4 January 2010; published 27 April 2010)

The triply differential cross section of ionization excitation of helium, leaving the residual ion in the $n = 2$ excited states, is evaluated for the kinematics considered experimentally by Dupré *et al.* [J. Phys. B **25**, 259 (1992)]. The interaction of the incident electron with the target is described at the first order, while the interaction of the ejected electron with the residual ion is treated very accurately within the formalism of the Jacobi matrix method. In the quasiphoton limit and for low ejected electron energies, the presence of series of doubly excited states, mainly below the $n = 3$ single ionization threshold in helium, makes the triply differential cross sections extremely sensitive to both the energy and the emission angle of the ejected electron. We show that the convolution of our results with a Gaussian energy profile, in which the full width at half-maximum corresponds to the energy resolution in the experiment, has a significant effect. Our results suggest that it is also important to account for the finite resolution on the measurement of the scattering angle when the experimental data are compared to the theoretical predictions. Comparison of our theoretical results convoluted both in energy and in angle with the experimental data demonstrates the importance of an accurate description of the helium spectrum. A possible two-step mechanism involving single ionization of the target followed by excitation of the core electron is proposed to explain the remaining discrepancies.

DOI: 10.1103/PhysRevA.81.042712 PACS number(s): 34.80.Dp, 34.80.Pa

I. INTRODUCTION

The simultaneous ionization excitation of helium by fast electron impact is a highly correlated process which has posed considerable challenge to both experiment and theory in recent years. Despite significant progress in our understanding of this process, there are still large and unexplained discrepancies between experiment and theory for certain kinematics. In this contribution, we focus on the strongly asymmetric coplanar kinematics used in the experiment by Dupré *et al.* [1] and calculate the triply differential cross section of ionization excitation of helium leaving He^+ in the excited $n = 2$ states.

In the experiment by Dupré *et al.* [1], the scattered electron energy was fixed at 5.5 keV. Three values of the ejected electron energy were considered, namely, 5, 10, and 75 eV, while the corresponding scattering angles are 0.35°, 0.32°, and 1°, respectively. In these kinematics, the amount of momentum transferred to the target is very small (large impact parameter), meaning that the dipolar or quasiphoton limit is approached. Moreover, for ejected electron energies of 5 and 10 eV, exit channels involving series of doubly excited states of helium are accessible. This and the fact that the energy and angular resolution in the experiment are relatively low make the comparison between theory and experiment rather delicate.

From the theoretical point of view, we can distinguish two types of calculations, depending on whether or not the exit channels involving doubly excited states of helium are included. In the experiment by Dupré *et al.* [1], the energy resolution varies from 4 to 5 eV. It is therefore expected that the effects of the doubly excited states of helium are washed out when the ejected electron energy is equal to 5 or 10 eV. This is the reason why, in the first type of calculation, doubly excited states of helium are fully neglected. Calculations based on this assumption involve first Born [2–4] and second Born [2,3,5] approaches. All these second Born calculations rely on the closure approximation [2,3,5] and its variants. Note, however, that a second-order distorted-wave calculation was performed by Chen and Madison [6] without making the closure approximation. They used a small but complete set of pseudostates to perform the sum over the intermediate states of the target. Regarding the second type of calculation, Fang and Bartschat [7,8] are the only ones who have performed first- and second-order calculations involving the contribution of doubly excited states. In particular, they considered the 10-eV ejected electron energy case.

In the case of kinematics involving relatively large momentum transfers, it is undeniable that the inclusion of second-order effects [2,3,5,7] improves the theoretical predictions significantly. However, the comparison between these predictions and the experimental data obtained by Stefani *et al.* [9], Bellm *et al.* [10,11], Dürr *et al.* [12], Rouvellou *et al.* [13], and Dogan and Crowe [14] shows that the agreement is far from being perfect. On the one hand, higher-order contributions could be significant. On the other hand, and despite efforts to go beyond the closure approximation [6], an accurate calculation of the second Born term remains an important challenge.

For very low-momentum transfers, it is legitimate to question the importance of second-order effects. It is interesting to note that, for an ejected electron energy of 75 eV in the experiments by Dupré *et al.* [1], second-order effects were negligible [2,3,5,7]. All first-order calculations agree very well with the experimental data. In that case, however, the exit channels that lead to the autoionization of helium are not directly accessible. The situation changes dramatically when the electron is ejected with energies equal to 5 or

*bernard.piraux@uclouvain.be

10 eV. Despite a slight improvement due to the inclusion of second-order effects, the agreement between the experimental data of Dupré *et al.* [1] and the theoretical predictions remains very poor. Fang and Bartschat [8] pointed out that, in addition to the correct description of the autoionization channels, the finite energy and angular resolution in the experiment require the convolution of the theoretical triply differential cross section (TDCS) with the response function of the detectors. In their calculations, they convoluted the TDCS at 10 eV with a Gaussian energy profile of 400 meV full width at half-maximum.

In this contribution, we calculate the ionization excitation TDCS in helium for all kinematics considered in the experiment by Dupré *et al.* [1]. As the first step, we treat the problem within the first-order Born approximation. The helium ground-state wave function is calculated accurately by means of a spectral method which has been described in great detail by Foumouo *et al.* [15]. The final single-continuum state is generated by means of the Jacobi matrix method [16,17]. This method provides a fully correlated multichannel scattering wave function which takes into account accurately electron correlations and, in particular, the contribution of the doubly excited states of helium. Moreover, for the ejected electron energies of 5 and 10 eV, we take into account the finite energy and angular resolution given in the experiment by convolution with the corresponding Gaussian profiles.

The organization of this paper is as follows. Section II describes the essentials of the theory. In Sec. III, we present and discuss our results for the TDCS for all kinematics considered experimentally by Dupré *et al.* [1]. The last section is devoted to the conclusion and perspectives. Atomic units are used throughout, unless otherwise stated explicitly.

II. THEORY

We consider the electron-impact ionization excitation of helium initially in its ground state, with the residual ion He^+ left in the $n = 2$ states. In this process, E_i and $\vec{k}_i$ are the energy and the momentum of the incident electron, which we assumed to be fast. The quantization axis coincides with the direction of this incident electron. After the collision, the scattered and ejected electrons have energies E_f and E_e and momenta $\vec{k}_f$ and $\vec{k}_e$, respectively. They emerge into the solid angles $d\Omega_f$ and $d\Omega_e$ centered about the directions (θ_f,ϕ_f) and (θ_e,ϕ_e). The TDCS for ionization excitation of helium is written as

$$\frac{d^3\sigma}{dE d\Omega_e d\Omega_f} = (2\pi)^4 \frac{k_e k_f}{k_i} |T_{fi}|^2, \tag{1}$$

where T_{fi} is the transition matrix element. Under the present conditions, we neglect the exchange of the incident electron with the target electrons and calculate the transition matrix element within the first Born approximation:

$$T_{fi}^{(1)} = -\frac{1}{(2\pi)^3} \langle e^{i\vec{k}_f\cdot\vec{r}_1} \Psi_f(\vec{r}_2,\vec{r}_3) | V | e^{i\vec{k}_i\cdot\vec{r}_1} \Psi_i(\vec{r}_2,\vec{r}_3) \rangle, \tag{2}$$

where $\Psi_i(\vec{r}_2,\vec{r}_3)$ and $\Psi_f(\vec{r}_2,\vec{r}_3)$ are the initial and final wave functions of helium, and V is given by

$$V = -\frac{2}{r_1} + \frac{1}{|\vec{r}_1 - \vec{r}_2|} + \frac{1}{|\vec{r}_2 - \vec{r}_3|}, \tag{3}$$

where $\vec{r}_1$, $\vec{r}_2$, and $\vec{r}_3$ are the position vectors of the projectile and the two target electrons, respectively. By integrating over $\vec{r}_1$ and by using the Bethe relation [18], we obtain

$$T_{fi}^{(1)} = -\frac{1}{(\pi K)^2} \langle \Psi_f(\vec{r}_2,\vec{r}_3) | (-1 + e^{i\vec{K}\cdot\vec{r}_2}) | \Psi_i(\vec{r}_2,\vec{r}_3) \rangle, \tag{4}$$

where $\vec{K} = \vec{k}_i - \vec{k}_f$ is the momentum transfer. Note that in the present case, the magnitude of this momentum transfer is much less than 1. In the next two subsections, we describe briefly the method used to generate the wave function of any bound state and single continuum of helium.

A. Helium bound-state wave functions

The calculation of the bound-state wave functions of helium is based on a spectral method of configuration interaction (CI) type. It consists in expanding the wave function in a finite basis of symmetrized products of discrete hydrogenlike functions for the radial coordinates and bipolar harmonics for the angular coordinates. For a given value of L, the total angular momentum of helium and M, its projection on the quantization axis, the bound-state wave function of energy E_α is written

$$\Theta_\alpha^{L,M}(\vec{r}_2,\vec{r}_3) = \sum_{LM} \sum_{l_2 l_3} \sum_{n_2 n_3} \beta_{n_2 n_3}^{l_2 l_3} \psi_{n_2 n_3}^{l_2 l_3 LM} \times \mathcal{A} \left(\frac{S_{n_3 l_3}^{\kappa_3}(r_3)}{r_3} \Lambda_{l_2 l_3}^{LM}(\hat{r}_2,\hat{r}_3) \frac{S_{n_2 l_2}^{\kappa_2}(r_2)}{r_2} \right), \tag{5}$$

where $\psi_{n_2 n_3}^{l_2 l_3 LM}$ is the expansion coefficient. $\mathcal{A}$ projects onto either singlet or triplet states to ensure the symmetry or antisymmetry of the spatial wave function as required by the Pauli principle. The coefficient $\beta_{n_2 n_3}^{l_2 l_3} = 1 + (1/\sqrt{2} - 1)\delta_{n_2 n_3}^{l_2 l_3}$ controls the redundancies which, from the exchange of the electrons, may occur in the basis. The radial hydrogenlike functions $S_{nl}^{\kappa}(r)$ are Coulomb-Sturmian functions defined for a given angular momentum l and radial index n by

$$S_{nl}^{\kappa}(r) = N_{nl}^{\kappa}\, r^{l+1} e^{-\kappa r} L_{n-l-1}^{2l+1}(2\kappa r), \tag{6}$$

where κ is a dilation parameter and $L_{n-l-1}^{2l+1}(2\kappa r)$ a Laguerre polynomial. The normalization constant given by

$$N_{nl} = \sqrt{\frac{\kappa}{n}} (2\kappa)^{l+1} \left(\frac{(n-l-1)!}{(n+l)!} \right)^{1/2} \tag{7}$$

is derived from the condition $\int_0^\infty S_{n,l}^{\kappa}(r) S_{n,l}^{\kappa}(r) dr = 1$. The radial index n is a positive integer satisfying $n \geqslant l+1$. The Coulomb-Sturmian functions are solutions of the Sturm-Liouville problem:

$$\left(-\frac{1}{2}\frac{d^2}{dr^2} + \frac{l(l+1)}{2r^2} - \frac{\xi}{r} + \frac{\kappa^2}{2} \right) S_{n,l}^{\kappa}(r) = 0, \tag{8}$$

with the associated boundary conditions $S_{n,l}^{\kappa}(0) = 0$ and $S_{n,l}^{\kappa}(\infty) = 0$. $\xi = \kappa n$ is the eigenvalue and κ is fixed and real. As a result, the Coulomb-Sturmian functions form a complete and discrete basis of square integrable functions. Note that they are exact solutions of the Schrödinger equation for a single electron in the Coulomb field of a nucleus of charge Z: when $\kappa = Z/n$, the Coulomb-Sturmian function $S_{n,l}^{\kappa}(r)$ coincides

with the hydrogenic bound state of principal quantum number n and angular quantum number l.

The angular part of the expansion (5) is expressed in terms of bipolar harmonics:

$$\Lambda^{LM}_{l_2,l_3}(\hat{r}_1,\hat{r}_2) = \sum_{m_2,m_3} \langle l_2 m_2 l_3 m_3 | LM\rangle Y_{l_2,m_2}(\hat{r}_1) Y_{l_3,m_3}(\hat{r}_2), \quad (9)$$

which couple the two individual electron angular momenta l_1 and l_2 in the L-S scheme. $Y_{l,m}(\hat{r})$ denotes a spherical harmonic, and $\langle l_2 m_2 l_3 m_3 | LM\rangle$ is a Clebsch-Gordan coefficient [19]. To preserve parity, which is a good quantum number, the L-S coupled individual angular momenta of the electrons must satisfy $(-1)^L = (-1)^{l_2+l_3}$.

The expansion coefficients $\psi^{l_2 l_3 LM}_{n_2 n_3}$ are obtained by imposing that the wave function is a solution of the time-independent Schrödinger equation. In fact, by performing a single diagonalization of the atomic Hamiltonian for each value of the total angular momentum L, we obtain discrete eigenenergies corresponding to bound states and to pseudostates representing the continuum. In the present case, we use 30 Coulomb-Sturmian functions per electron and per pair of individual electron angular momenta. For $L = 0$, the number of these pairs is 4. This gives a ground-state energy of -2.9033 a.u., compared to $-2.903\,724\,377\,0$ a.u., the reference data of Drake [20]. The fact that our CI approach does not fulfill the Kato cusp condition associated with two-electron coalescence limits the accuracy of the ground-state energy of helium. For excited bound states, however, the Kato cusp condition plays a minor role and the accuracy of the energy increases rapidly with the degree of excitation. This requires, however, the introduction of various sets of dilation parameters [15].

The method described above to generate the bound states of helium can also be used to evaluate the energy and width of the doubly excited states. This is done by performing a complex dilation of the atomic Hamiltonian [15].

B. Helium single-continuum wave functions

We describe the single continuum of helium by a multichannel scattering wave function. This wave function can be generated accurately with the so-called Jacobi- or J-matrix method. This method, which is of spectral type, bears a close resemblance to the R-matrix theory. As in the latter case, the configuration space is divided into two regions. In the inner region, the space is spanned by the same finite Coulomb-Sturmian basis used to generate the bound states of the Hamiltonian. In the outer region, it is assumed that the outgoing electron moves in a screened Coulomb potential. To reproduce correctly the asymptotic behavior of the outgoing electron wave function in each channel, it is expanded in an infinite basis of Coulomb-Sturmian functions.

For a given channel Γ, and a given total energy E of the final state, this single-continuum wave function reads as

$$\Xi_\Gamma(\vec{r}_2,\vec{r}_3) = \sum_\alpha b^\Gamma_\alpha(E,\hat{k}_e)\Theta^{L,M}_\alpha(\vec{r}_2,\vec{r}_3) + \sum_{\Gamma'}\sum_{n'} f^{\Gamma'\Gamma}_{n'}(E,\hat{k}_e)\Phi^{\Gamma'}_{n'}(\vec{r}_2,\vec{r}_3). \quad (10)$$

The channel $\Gamma \equiv (\nu,\lambda,l;L,M)$ is characterized by a given value of the target radial and angular quantum numbers, the angular momentum of the ejected electron, and the target total angular momentum and its projection, respectively. The right-hand side of expression (10) contains two terms. The first is the representation of the scattering wave function in the inner region, while the second term accurately describes its asymptotic behavior. It is a double expansion over all included channels and over n', the radial index of the Coulomb-Sturmian functions describing the ejected electron. $\Phi^{\Gamma'}_{n'}(\vec{r}_2,\vec{r}_3)$ is the two-electron wave function in the outer region. It is given by

$$\Phi^{\Gamma'}_{n'}(\vec{r}_2,\vec{r}_3) = \mathcal{A}\left(\frac{\chi_{\nu'\lambda'}(r_3)}{r_3}\Lambda^{L'M'}_{\lambda' l'}(\hat{r}_2,\hat{r}_3)\frac{S^{\kappa_2}_{n' l'}(r_2)}{r_2}\right), \quad (11)$$

where $\chi_{\nu'\lambda'}(r_3)$ is the wave function associated with the bound states and the pseudostates representing the continuum of the residual ion. It is obtained by diagonalizing the Hamiltonian associated with He^+ in our finite Coulomb-Sturmian basis. By demanding that $\Xi_\Gamma(\vec{r}_2,\vec{r}_3)$ satisfies the Schrödinger equation, we obtain an algebraic system of equations to solve for the coefficients $b^\Gamma_\alpha(E,\hat{k}_e)$ and $f^{\Gamma'\Gamma}_{n'}(E,\hat{k}_e)$. The outer-region expansion coefficients are written as follows:

$$f^{\Gamma'\Gamma}_{n'}(E,\hat{k}_e) = f^{\Gamma'\Gamma}_{n'}(E)\sum_{\mu' m'}\langle \lambda'\mu' l' m' | LM\rangle y^*_{l'm'}(\hat{k}_e), \quad (12)$$

where

$$f^{\Gamma'\Gamma}_{n'}(E) = \tau^{l'_2}_{n'}(E-\epsilon)\delta_{\Gamma\Gamma'} - \Omega^{l'_2}_{n'}(E-\epsilon)T_{\Gamma\Gamma'}. \quad (13)$$

In this expression, l'_2 refers to channel Γ' and ϵ is the energy of the target electron. $\tau^{l'_2}_{n'}$ is the coefficient of the expansion of the regular Coulomb wave in Coulomb-Sturmian functions, while $\Omega^{l'_2}_{n'}$ is the expansion coefficient of either an outgoing Coulomb wave for open channels or a dying exponential for closed channels. It is important to stress that all closed channels do contribute to the transition matrix $T_{\Gamma\Gamma'}$. Let us also mention that the double-continuum channels are treated in an approximated way. Asymptotically, the outer electron is described by a Coulomb wave, and the inner one by a pseudostate. In the inner region, however, we stress that the double continuum is correctly described.

The reliability of the J-matrix approach has been tested in numerous cases [15]. In the present contribution, the convergence of our results is tested against the number of Sturmian functions and the number of pairs (λ,l) of individual electron angular momenta for several fixed values of both the energy and the emission angle of the ejected electron. We actually included 50 Coulomb-Sturmian functions per electron and per pair (λ,l). We take into account six values (from 0 to 5) of the total angular momentum L and at least four pairs (λ,l) per L. Under these conditions, the number of channels included in the single-continuum wave function is about 350 for a given L. It is important to note that in the present case, there is no restriction on the parity of the final-state wave function: states of natural and unnatural parity are included. Note that within our first-order treatment of the collision, states of unnatural parity are not expected to play a significant role in the quasiphoton limit.

To check the computer code, we proceeded as follows. We calculated, both analytically and numerically, the TDCS for electron-impact single ionization of helium. In this calculation, the ground-state wave function is the Sturmian expansion

of the Byron and Joachain wave function [21], which is an analytical fit to the Hartree-Fock wave function, while the final state is taken as the Sturmian expansion of a symmetrized product of the He^+ ground-state wave function for the bound electron times a Coulomb wave with an effective charge $Z = 1$. We obtain in this case a perfect agreement between the analytical and the numerical results. Ionization excitation has also been considered in this way by replacing the He^+ ground-state wave function by the wave function of some excited states. We also get an excellent agreement between both the analytical and the numerical calculations.

III. RESULTS

We begin our discussion by considering the TDCS for the kinematics in which $E_i = 5640.41$ eV, $E_f = 5500$ eV, $E_e = 75$ eV, and $\theta_f = 1^\circ$. This corresponds to a momentum transfer of 0.44 a.u. In Fig. 1, we compare our first-order results to the experimental results of Dupré *et al.* [1] and to other first Born results. They include the close-coupling calculations of Marchalant *et al.* [2], the convergent-close-coupling calculations of Kheifets *et al.* [4], the R-matrix with pseudostates method of Fang and Bartschat [7], and the Faddeev-Merkuriev-Jacobi matrix approach of Zaytsev *et al.* [22]. All first Born results are in fair or excellent agreement with the experimental data. Fang and Bartschat [7], Marchalant *et al.* [3], and Kheifets *et al.* [5] evaluated the second-order contributions. Their results clearly show that the corresponding effect is very small for this type of kinematics. In fact, the TDCS exhibits a behavior which is very similar to that of the corresponding TDCS for single ionization of helium without excitation of the residual ion in the limit of very small momentum transfers, namely, two peaks along the direction of the momentum transfer, with the binary peak higher than the recoil one.

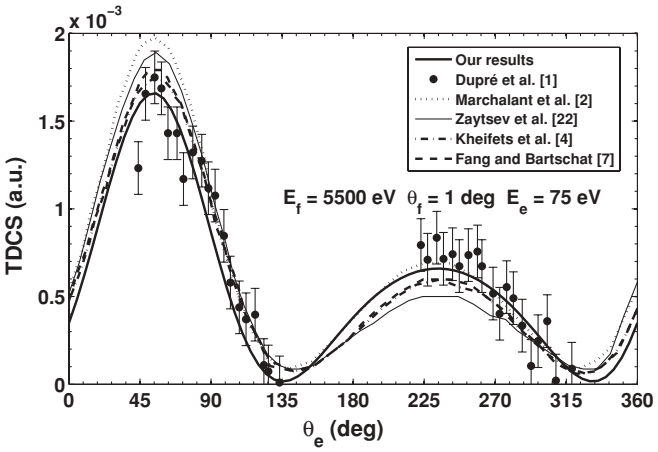

FIG. 1. Triply differential cross section for electron-impact ionization excitation of He in its ground state, leaving He^+ in the $n = 2$ states, as a function of the ejected electron angle θ_e. The incident electron energy $E_i = 5640.41$ eV, the scattered electron energy $E_f = 5500$ eV, and the ejected electron energy $E_e = 75$ eV. The scattering angle is $\theta_f = 1^\circ$. Filled circles are the experimental results of Dupré *et al.* [1]. Our first-order result is the bold solid line. These are compared to the first Born results of Fang and Bartschat [7] (dashed line), Kheifets *et al.* [4] (dot-dashed line), Marchalant *et al.* [2] (dotted line), and Zaytsev *et al.* [22] (thin solid line).

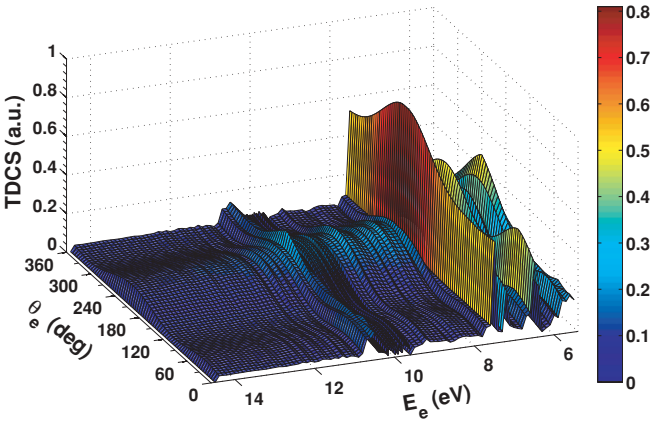

FIG. 2. (Color online) Triply differential cross section for electron-impact ionization excitation of He in its ground state, leaving He^+ in the $n = 2$ states, as a function of the ejected electron energy E_e and angle θ_e. The scattered electron energy $E_f = 5500$ eV and the scattering angle $\theta_f = 0.32^\circ$.

The situation changes dramatically for very low energies of the ejected electron, where exit channels involving doubly excited states of helium are directly accessible. Whether or not the inclusion of the second-order contribution is decisive is still an open question, which is addressed later. It is clear, however, that it is crucial to describe accurately the target electron correlations. We show this by considering the two other kinematics that have been studied experimentally by Dupré *et al.* [1], namely, ($E_i = 5570.41$ eV, $E_f = 5500$ eV, $E_e = 5$ eV, $\theta_f = 0.35^\circ$) and ($E_i = 5575.41$ eV, $E_f = 5500$ eV, $E_e = 10$ eV, $\theta_f = 0.32^\circ$). It is important to stress that our J-matrix calculation of the final single-continuum wave function takes accurately into account the presence of various series of doubly excited states of helium. Figures 2 and 3 show three-dimensional graphs of the TDCS as a function of both the ejection angle θ_e and the ejected electron energy for these two kinematics. Figure 2 shows the TDCS for an ejected electron energy around 10 eV. In the region very close to $E_e = 10$ eV, the TDCS exhibits moderate variations due to the presence of

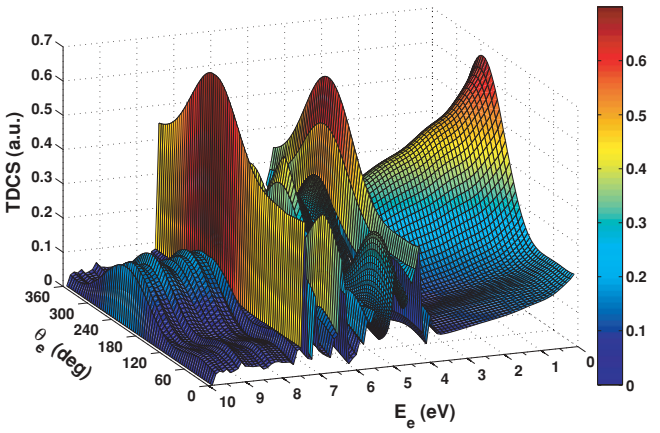

FIG. 3. (Color online) Same as Fig. 2, for the same scattered electron energy, $E_f = 5500$ eV, and a scattering angle $\theta_f = 0.35^\circ$.

the doubly excited states above the $n = 3$ threshold. However, at the $n = 3$ threshold ($E_e = 7.54$ eV) and below, very sharp variations occur. Below the $n = 3$ threshold, these sharp resonances are due to $L = 1$ and $L = 2$ doubly excited states. Given the finite-energy resolution of 4.2 eV in the experiment, this region of resonances should also contribute significantly to the experimental cross section. As shown in Fig. 3, the presence of very sharp variations is even more pronounced in the case where the ejected electron energy is around 5 eV. In that case, we also see a strong effect of the $n = 2$ threshold in the large energy interval from 0.1 to about 4.4 eV. Above this, the sharp variations in the TDCS are due to the same resonances as mentioned previously for the 10-eV case. To illustrate the high sensitivity of the TDCS to the ejected electron energy, Fig. 4 shows the ejected-electron energy dependence of the TDCS in a narrow interval around 10 eV [Fig. 4(a)] and 5 eV [Fig. 4(b)] for two fixed values of the ejection angle close to the position of the binary and recoil peaks, respectively.

As mentioned by Fang and Bartschat [8], comparison of the theoretical predictions with the experimental data requires a convolution of the theoretical results with the response function of the detector. By means of their second Born treatment, they calculated the TDCS in the case where the ejected-electron energy is equal to 10 eV and convoluted their results with a Gaussian energy profile of width 400 meV. Such a width, however, does not include the sharp variations of the TDCS around $E_e = 7$ eV, which, given the experimental energy resolution of 4.2 eV, should contribute.

In the following, we analyze the convolution of our results in energy for the $E_e = 10$ eV case and in both energy and angle for $E_e = 5$ eV. Note that the convolution of our results in energy and/or in angle requires an enormous amount of numerical calculations. This is the main reason why the angular convolution was performed only in the $E_e = 5$ eV case, which has not been treated before. We convolute our results in energy with a Gaussian profile of width 4.2 eV, which is the energy resolution of the experiment by Dupré *et al.* [1]. The results are presented in Fig. 5 for $E_e = 10$ eV. In Fig. 5(a), we show

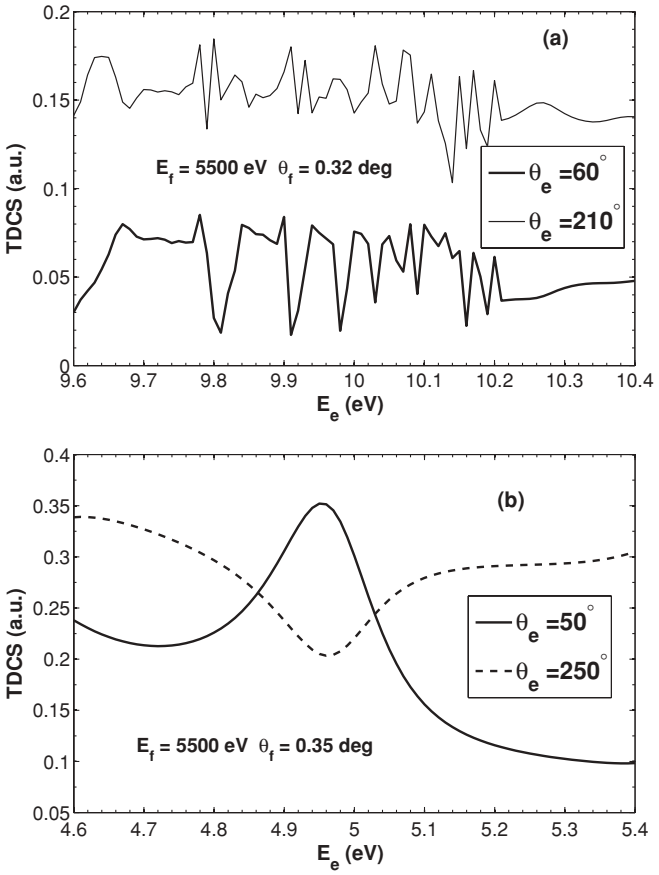

FIG. 4. Ejected-electron energy dependence of the triply differential cross section of electron-impact ionization excitation of helium leaving the residual ion in the excited $n = 2$ states. Two kinematics are considered: (a) ejected-electron energy E_e around 10 eV, scattered-electron energy $E_f = 5500$ eV, and scattering angle $\theta_f = 0.32^\circ$ and (b) ejected-electron energy E_e around 5 eV, scattered-electron energy $E_f = 5500$ eV, and scattering angle $\theta_f = 0.35^\circ$. In each case, two values of the ejection angle, close to the positions of the binary and recoil peaks, are chosen.

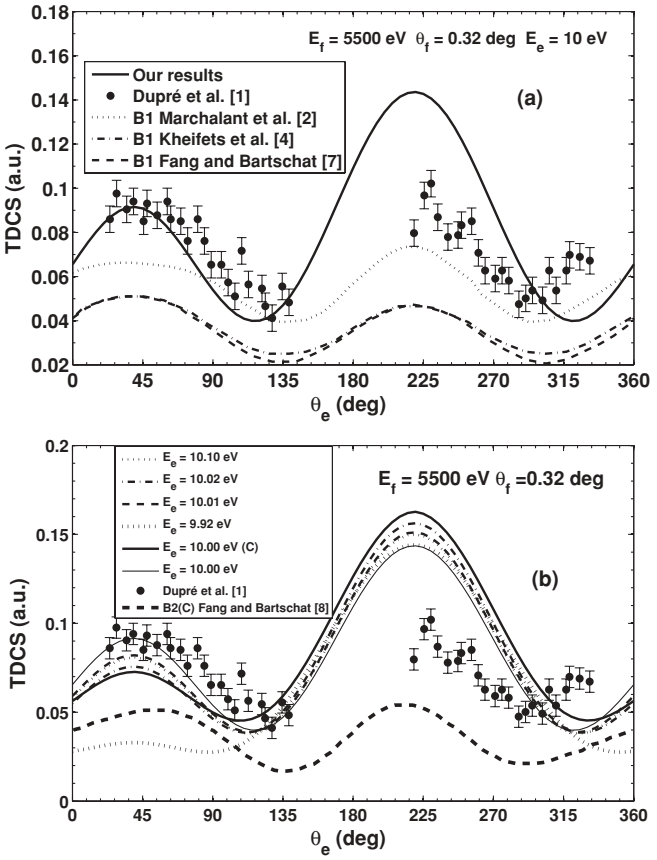

FIG. 5. Ejection angle dependence of the triply differential cross section of electron-impact ionization excitation of helium, leaving the residual ion in the excited $n = 2$ states, for a kinematics in which the scattered-electron energy is $E_f = 5500$ eV and the scattering angle, $\theta_f = 0.32^\circ$. (a) For a fixed value of the ejected-electron energy of 10 eV, our uncovoluted result (bold solid line) is compared to the experimental data of Dupré *et al.* [1] and to the first Born results of Marchalant *et al.* (dotted line) [2], Kheifets *et al.* (dot-dashed line) [4], and Fang and Bartschat (dashed line) [7]. (b) Our data for various ejected-electron energies and our energy-convoluted result [bold solid line labeled (C)] obtained with a Gaussian profile of width 4.2 eV are compared to the same experimental data and to the convoluted second-order results (thick dashed line) of Fang and Bartschat [8].

our unconvoluted results compared to the first Born results of Marchalant *et al.* [2], Kheifets *et al.* [4], and Fang and Bartschat [7]. Our results are systematically above the other first-order predictions and in fair agreement with the experimental data, in particular, around the binary peak. The second-order results of Marchalant *et al.* [3], Kheifets *et al.* [5], and Fang and Bartschat [7,8] are in better agreement with the experimental data than their respective first-order results. In Fig. 5(b), we show the TDCS for various energies of the ejected electron as well as the result of the energy convolution. These data are compared to the convoluted second-order results of Fang and Bartschat [8] and to the same experimental results. The fact that the convoluted second-order results of Fang and Bartschat are systematically below our first-order convoluted data is intriguing. This might be related to the number of channels taken into account in our final-state wave function, which is much higher than in the calculations of Fang and Bartschat. Surprisingly, the agreement of our energy-convoluted results with the experimental data deteriorates, although our results are still above all the other first and second Born predictions. We actually see two possible reasons to explain this effect. First, it is possible that some resonances between the $n = 2$ and the $n = 3$ thresholds are not resolved with our basis due to its finite size. In particular, we expect that the inclusion of many pairs (λ,l) of individual electron angular momenta is necessary to reproduce the spectrum of helium in this region accurately [23]. This suggests that a detailed study of the helium resonances and convergence tests of the TDCS for many values of the ejected electron parameters are necessary. This detailed study can be performed with our approach but requires enormous computational resources not yet available. In the present calculations, we do observe a convergence of the TDCS against the number of pairs (λ,l) but for values of the ejected electron energy of 75 and 10 eV. Note that in the latter case, the energy convolution requires the calculation of the TDCS for ejected electron energies ranging from 14 to 6 eV, with a very thin energy discretization in the region of the resonances.

The second reason is related to the inclusion of the second-order contributions. The fact that the amplitude of the recoil peak is higher than the amplitude of the binary one suggests that second-order effects are indeed important. The previous discussion clearly demonstrates that within a second Born treatment, an accurate description of the resonances is necessary. Moreover, it is not clear whether the closure approximation is still valid. Indeed, we could imagine the following two-step mechanism: a first transition from the helium ground state to a single-continuum state, leaving the residual ion in its ground state (single ionization), followed by a second transition to another single-continuum state in which the bound electron is excited while the ejected one keeps the same energy (excitation of the electron core). It is important to realize that the coupling between two single continua can be very strong when the free electron has the same energy in both single continua. This and the fact that helium may reach its final continuum state via intermediate resonances prevent a second-order treatment where all intermediate states have the same weight (closure approximation). Instead, this treatment requires a very large number of intermediate target states to be taken into account accurately. Note that a similar

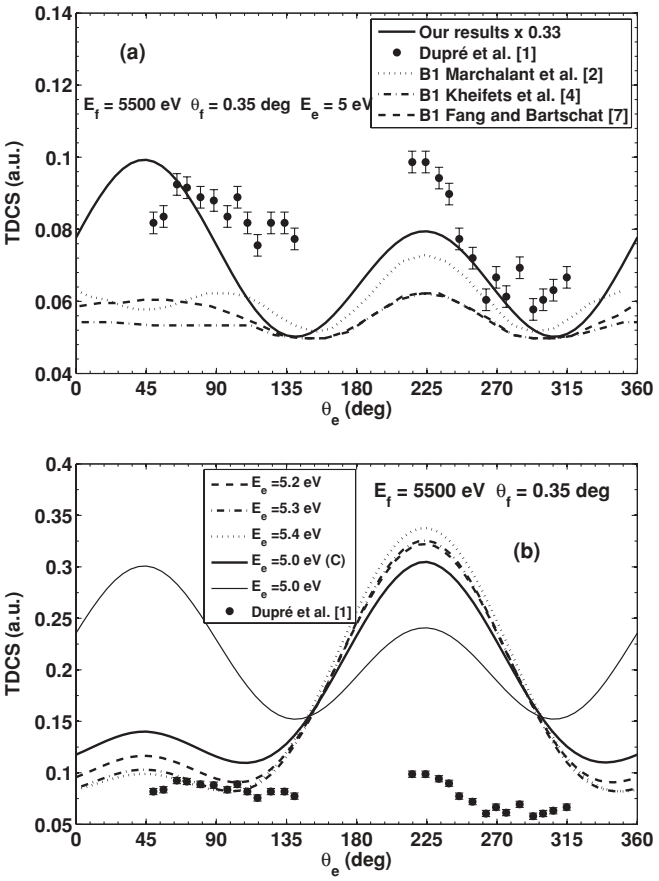

FIG. 6. Same as Fig. 5, for a scattering angle $\theta_f = 0.35^\circ$ and an ejected-electron energy equal to 5 eV (a) or about 5 eV (b).

second-order process involving the coupling of two single continua occurs in the case of two-photon ionization excitation of a two-electron system. Proulx *et al.* [24] have studied this process in the case of H^- and have shown that the coupling between the two single continua leads to a very strong effect due to the resonant excitation of the core electron.

Let us now consider Fig. 6. In Fig. 6(a), we show our unconvoluted result for an energy of the ejected electron of 5 eV and compare it to both the experimental data of Dupré *et al.* [1] and the first Born results of Marchalant *et al.* [2], Kheifets *et al.* [4], and Fang and Bartschat [7]. Our unconvoluted results are significantly higher than both the experimental data and the other theoretical predictions. However, it is important to bear in mind that for an energy of 5 eV, the many resonances between the $n = 2$ and the $n = 3$ thresholds play a role in making the TDCS extremely difficult to calculate. Figure 6(b) shows our energy-convoluted results. As expected, the effect is extremely important: in the region of the binary peak, the convoluted results get much closer to the experimental data but stay higher than both the experimental data and the other theoretical predictions. Around the recoil peak, the gap between the experimental data and our predictions increases. In Fig. 7, we show our energy-convoluted result for the TDCS as a function of the angle of the ejected electron for various scattering angles. Clearly, the TDCS varies significantly in amplitude and the position of both peaks changes as expected. After the convolution on the

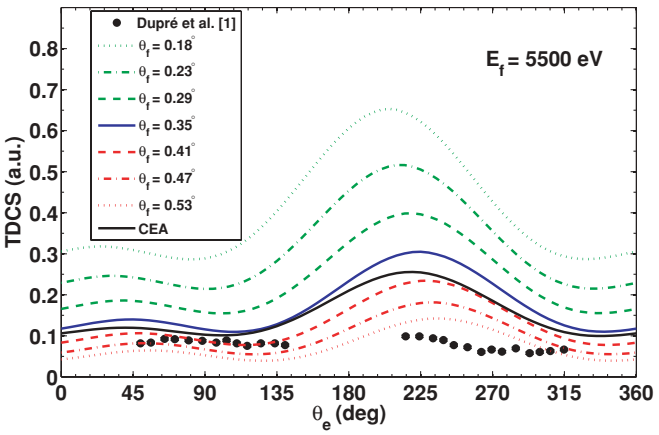

FIG. 7. (Color online) Ejection angle dependence of the triply differential cross section of electron-impact ionization excitation of helium, leaving the residual ion in the excited $n = 2$ states, for a kinematics in which the scattered-electron energy is $E_f = 5500$ eV. Our energy-convoluted data (curves labeled CE) are given for various scattering angles θ_f between 0.17° and 0.53°. Our angle- and energy-convoluted result is the bold solid line labeled CEA. We use a Gaussian profile of width 0.36° for the convolution on the scattering angles. These results are compared to the experimental data of Dupré *et al.* [1].

scattering angles with a Gaussian profile of width 0.36°, which corresponds to the experimental resolution, our results get even closer to the experimental data, in particular, around the binary peak. However, important discrepancies subsist regarding the position of the binary peak and the amplitude of the recoil peak. This suggests, again, that second-order effects must be important.

IV. CONCLUSION

In this contribution, we calculate the TDCS of ionization excitation of helium by impact of fast electrons. The interaction of the incident electron with helium is treated at the first order, while electron correlations in the target are accurately described by means of a spectral method that includes a Jacobi-matrix treatment of the multichannel scattering wave function of the final single continuum. Our results are compared to the experimental data of Dupré *et al.* In the case where the ejected electron has an energy of 75 eV, the agreement between our first-order results and the experimental data is excellent. Moreover, our results also agree with the other first- and second-order predictions. This means that in this quasiphoton regime, the second-order results are negligible as expected. However, for much lower ejection energies, between 5 and 13.6 eV, the situation changes dramatically. In this case, exit channels leading to autoionization of helium are directly accessible. At an ejection energy of 10 eV, our first-order results get very close to the experimental data and, in fact, closer than the other first- and second-order results in the vicinity of the binary peak. However, if the theoretical data are convoluted in energy with a Gaussian profile whose width at half maximum is equal to the experimental resolution, the results change significantly. The fact that the effect of the convolution is so important is attributed to the presence of doubly excited states below the $n = 3$ threshold and to the presence of the $n = 3$ threshold itself. By contrast, the doubly excited states above the $n = 3$ threshold do not influence the results significantly. Nevertheless, it is surprising that the agreement between the experimental data and our results deteriorates once the energy convolution is performed. This suggests that second-order contributions are important. However, our results clearly show that such calculation should include an accurate description of many doubly excited states and go beyond the closure approximation, which still represents a challenge. For an ejection energy of 5 eV, our unconvoluted first-order results are too high compared to the experimental results. In this case, the presence of the second and the third thresholds, and the doubly excited states between them, makes the TDCS extremely sensitive to both the energy and the angle of the ejected electron. The energy convolution of our results improves the agreement with the experimental data in the region of the binary peak, while the opposite is observed around the recoil peak. On the other hand, we show that the triply differential cross section is also very sensitive to the value of the scattering angle. This led us to convolute our results in both energy and angle. This, however, is not sufficient to explain the remaining discrepancies between theory and experiment. We propose a two-step mechanism involving a transition between two single-continuum states in which the bound electron of the residual ion may be resonantly excited.

ACKNOWLEDGMENTS

The authors enjoyed very interesting discussions with Johannes Eiglsperger, Javier Madroñero, and Yuri Popov. They gratefully acknowledge the financial support of the IISN (Institut Interuniversitaire des Sciences Nuclaires) through Contract No. 4.4.503.02.F, as well as the financial support of the FRFC (Fonds de la Recherche Fondamentale et Collective) through Contract No. 2.4.592.07.F. J.M.N.D. is indebted to the Abdus Salam International Centre for Theoretical Physics (ICTP, Italy) for its support through the OEA-AC-71 Project and the Associateship Office. The authors thank the Université catholique de Louvain for providing them access to the supercomputer of the CISM (Calcul Intensif et Stockage de Masse), which is supported by the FNRS (Fonds National de la Recherche Scientifique) through FRFC Project No 2.4556.99.

[1] C. Dupré, A. Lahmam-Bennani, A. Duguet, F. Mota-Furtado, P. F. O'Mahony, and C. Dal Capello, J. Phys. B **25**, 259 (1992).
[2] P. J. Marchalant, Colm T. Whelan, and H. R. J. Walters, J. Phys. B **31**, 1141 (1998).
[3] P. J. Marchalant, J. Rasch, C. T. Whelan, D. H. Madison, and H. R. J. Walters, J. Phys. B **32**, L705 (1999).
[4] A. S. Kheifets, I. Bray, and K. Bartschat, J. Phys. B **32**, L433 (1999).

[5] A. S. Kheifets, Phys. Rev. A **69**, 032712 (2004).
[6] Z. Chen and D. H. Madison, J. Phys. B **38**, 4195 (2005); Z. Chen, D. H. Madison, and K. Bartschat, *ibid.* **40**, 2333 (2007).
[7] Y. Fang and K. Bartschat, J. Phys. B **34**, L19 (2001).
[8] Y. Fang and K. Bartschat, Phys. Rev. A **64**, 020701(R) (2001).
[9] G. Stefani, L. Avaldi, and R. Camilloni, J. Phys. B **23**, L227 (1990).
[10] S. Bellm, J. Lower, and K. Bartschat, Phys. Rev. Lett. **96**, 223201 (2006).
[11] S. Bellm, J. Lower, K. Bartschat, X. Guan, D. Weflen, M. Foster, A. L. Harris, and D. H. Madison, Phys. Rev. A **75**, 042704 (2007).
[12] K. Bartschat, J. Phys.: Conf. Ser. **141**, 012002 (2008).
[13] B. Rouvellou, R. Rioual, A. Pochat, R. J. Tweed, J. Langois, G. Nguyen Vien, and O. Robaux, J. Phys. B **33**, L599 (2000).
[14] M. Dogan and A. Crowe, J. Phys. B **31**, 1611 (1998).
[15] E. Foumouo, G. Lagmago Kamta, G. Edah, and B. Piraux, Phys. Rev. A **74**, 063409 (2006).
[16] R. Gersbacher and J. T. Broad, J. Phys. B **23**, 365 (1990).
[17] H. A. Yamani and L. Fishman, J. Math. Phys. **16**, 410 (1975).
[18] I. S. Gradshteyn and I. M. Ryzhik, *Table of Integrals, Series and Products*, 5th ed. (Academic Press, San Diego, CA, 1994).
[19] D. A. Varshalovich, A. N. Moskalev, and V. K. Khersouskii, *Quantum Theory of Angular Momentum* (World Scientific, Singapore, 1988).
[20] G. W. F. Drake, *Handbook of Atomic, Molecular, and Optical Physics* (Springer, New York, 2006).
[21] F. W. Byron Jr. and C. J. Joachain, Phys. Rev. **146**, 1 (1966).
[22] S. A. Zaytsev, V. A. Knyr, Yu. V. Popov, and A. Lahmam-Bennani, Phys. Rev. A **75**, 022718 (2007).
[23] J. Eiglsperger, B. Piraux, and J. Madronero, Phys. Rev. A **80**, 022511 (2009).
[24] D. Proulx, M. Pont, and R. Shakeshaft, Phys. Rev. A **49**, 1208 (1994).